ELECTROSPINNING OF POLY (MMA-CO-MAA) COPOLYMERS AND THEIR LAYERED SILICATE NANOCOMPOSITES FOR IMPROVED THERMAL PROPERTIES

M. Wang* and G.C. Rutledge
Dept. of Chemical Engineering
Massachusetts Institute of Technology
Cambridge, MA 02139

Alex J. Hsieh
U.S. Army Research Laboratory
AMSRD-ARL-WM-MD
Aberdeen Proving Ground, MD 21005-5069

ABSTRACT

Copolymers consisting of methyl methacrylate (MMA) and methacrylic acid (MAA) and their layered silicate nanocomposites were electrospun to form fibers with diameters in the sub-micron range. The presence of MAA increased the glass transition temperature and thermal stability of the copolymers through formation of anhydrides upon heating. Dispersion of layered silicates within the nanocomposites improved the electrospinnability of the nanocomposite dispersions. Fibers of uniform diameters were obtained for the poly-(MMA-co-MAA) copolymers and their nanocomposites containing montmorillonite (MMT), while protrusions were observed on the electrospun fibers from nanocomposites containing fluorohectorite (FH). MMT is predominantly exfoliated and well distributed within the fiber and oriented along the fiber axis. The electrospinnability of copolymer solutions and nanocomposite dispersions predicted based on both rheological analyses and conductivity measurements correlates well with the experimental electrospinning observations. Char formation was observed when the MMT-containing fibers were heated above the decomposition temperature indicating the characteristics of reduced flammability and increased self-extinguishing properties.

1. INTRODUCTION

Electrospinning is an effective method for the production of polymeric fibers with diameters ranging from tens of nanometers to microns [Doshi et al., 1995]. This technique has attracted great interest over the last decade due to the potential applications of nanofibers (i.e. fibers with diameters below 100 nm) in such areas as molecular electronics, filtration, tissue engineering, sensors, protective clothing, and reinforcing components for nanocomposites. In electrospinning, a solidified fiber is formed from electrically charged polymer liquid jet in the presence of an external electric field. The electrically charged liquid jet accelerated by external electric field, travels in a straight line, then undergoes a whipping instability that leads to jet stretching before hits a grounded collector [Hohman et al., 2001a, 2001b; Reneker et al., 2000; Feng, 2002, Yarin et al., 2001; Yu et al., 2004]. "Electrospinnability" of a polymer solution is thus defined as the ability to form a continuous jet that is stable against breakup into droplets, in the presence of an electric field [Yu et al., 2004]. During the electrospinning process, a Rayleigh instability driven by the surface tension, which tends to break the jet into droplets, can develop along the thin liquid jet. This instability becomes more important as the diameter of the jet becomes smaller. The external electric field accelerates the electrically charged jet and stretches it along the field axis, while the repulsive forces resulting from the surface charges lead to bending of the jet and its stretching in the direction normal to the electric field. These two forces depend strongly on the volume charge density of the jet, with most of the charges believed to reside at the jet surface. External electric field, surface charges and solution elasticity tend to suppress the Rayleigh instability and stabilize the jet. As a result, the surface tension, the charge density and the solution elasticity are thought to play large roles in determining the electrospinnability of polymer solutions [Yu et al., 2004].

Incorporation of small levels of layered silicates (i.e. clays) into a polymer matrix has shown great promise of yielding nanocomposites with enhanced mechanical strength, chemical resistance, thermal stability, and self-extinguishing flammability characteristics compared to the pristine polymers [Usuki et al., 1993; Kojima et al., 1993; Giannelis, 1996]. These property improvements are attributed to the nanometric thickness and high aspect ratio of the individual clay platelets, as well as to the nanocomposite morphology with the platelets being exfoliated and well dispersed. The high aspect ratio of clay platelets allows their nanocomposites to form a percolated mesoscale-structure at low volume fraction. However, it is more difficult to achieve complete exfoliation for layered silicates with high aspect ratio [Gilman et al., 2000], which offsets some of the

1. REPORT DATE **00 DEC 2004**	2. REPORT TYPE **N/A**	3. DATES COVERED **-**

4. TITLE AND SUBTITLE	5a. CONTRACT NUMBER
Electrospinning Of Poly (Mma-Co-Maa) Copolymers And Their Layered Silicate Nanocomposites For Improved Thermal Properties	5b. GRANT NUMBER
	5c. PROGRAM ELEMENT NUMBER

6. AUTHOR(S)	5d. PROJECT NUMBER
	5e. TASK NUMBER
	5f. WORK UNIT NUMBER

7. PERFORMING ORGANIZATION NAME(S) AND ADDRESS(ES) **Dept. of Chemical Engineering Massachusetts Institute of Technology Cambridge, MA 02139; U.S. Army Research Laboratory AMSRD-ARL-WM-MD Aberdeen Proving Ground, MD 21005-5069**	8. PERFORMING ORGANIZATION REPORT NUMBER

9. SPONSORING/MONITORING AGENCY NAME(S) AND ADDRESS(ES)	10. SPONSOR/MONITOR'S ACRONYM(S)
	11. SPONSOR/MONITOR'S REPORT NUMBER(S)

12. DISTRIBUTION/AVAILABILITY STATEMENT
Approved for public release, distribution unlimited

13. SUPPLEMENTARY NOTES
See also ADM001736, Proceedings for the Army Science Conference (24th) Held on 29 November - 2 December 2005 in Orlando, Florida. , The original document contains color images.

14. ABSTRACT

15. SUBJECT TERMS

16. SECURITY CLASSIFICATION OF:			17. LIMITATION OF ABSTRACT	18. NUMBER OF PAGES	19a. NAME OF RESPONSIBLE PERSON
a. REPORT **unclassified**	b. ABSTRACT **unclassified**	c. THIS PAGE **unclassified**	**UU**	**8**	

advantages of working with these materials. The common approaches undertaken to achieve exfoliated nanocomposite structures include modification of the clay surface chemistry from hydrophilic to organophilic in order to improve compatibility with the host polymer matrix, as well as utilization of special processing techniques, such as in-situ polymerization, high shear solution blending or melt blending, to achieve delamination of the large stacks of silicate nanoparticles into isolated (i.e. exfoliated) platelets or "tactoids" consisting of only a small number of platelets.

The feasibility of incorporation of nanometer-sized particulates into fibers has made electrospinning even more attractive for the production of composite fibers [Wang et al., 2004a]. Orientation of the filler particles within the fibers during processing creates the possibility for manipulation of nanoparticles through appropriate handling of the fibers in which they are embedded and oriented. The critical material parameters for manufacturing such composite fibers include the type and geometry of the fillers, and the extent of homogeneous dispersion of filler within the polymer solution. Fong and coworkers first demonstrated the electrospinning of layered silicate nanocomposite into fibers [Fong et al., 2002]. They compounded nylon-6 with MMT by melt processing, and then used hexafluoro-2-propanol (HFIP) or a mixture of HFIP and dimethylformamide (DMF) to prepare nanocomposite dispersions for electrospinning. The degree of dispersion and morphology of MMT in the resulting fibers were characterized, but no fiber properties were reported.

The objective of this work is to utilize electrospinning for the development of poly (methyl methacrylate), PMMA, based fibers with improved thermal properties. Specifically, we describe the formation of fibers electrospun from solution of poly (MMA-co-MAA) copolymer (50/50 weight ratio of MMA and methacrylic acid, MAA) in dimethylformamide (DMF) and the corresponding layered-silicate nanocomposite dispersions. Two types of pristine clays, MMT and fluorohectorite (FH) without any organic modifiers, were used to study the effect of lateral dimension of the clay platelets on fiber formation. The electrospinnability of the polymer solutions and nanocomposite dispersions can be understood in terms of the extensional rheological properties and the conductivity of the solutions. The morphology and thermal properties of the fibers are also reported.

2. EXPERIMENTAL

2.1 Materials and Electrospinning

The poly (MMA-co-MAA) copolymers and their nanocomposites consisting of either montmorillonite (MMT) or fluorohectorite (FH) layered silicates prepared by emulsion polymerization were used in this study [Wang et al., 2004b]. For electrospinning, polymer solutions of 6 and 8 percent by weight were prepared by directly adding the neat polymers to the dimethylformamide (DMF). The solutions were vigorously stirred for at least 24 hours at room temperature. Nanocomposite dispersions were also prepared by adding nanocomposites at concentration of 6 and 8 weight percent in DMF. The dispersions were vigorously stirred for at least 72 hours at room temperature. A parallel-plate electrospinning apparatus was used in this study, as described by Shin et al. [Shin et al., 2001] and Fridrikh et al. [Fridrikh et al., 2003]. The electric field, solution flow rate and distance between the two parallel plates were adjusted to obtain a stable jet.

2.2 Solution rheology

Shear rheology was performed on an AR2000 Rheometer (TA Instruments) at 25ºC using parallel-plate geometry with 40 mm diameter plates. Steady shear measurements were carried out at constant shear rates ranging from 1 s^{-1} to 1000 s^{-1}. Extensional rheological measurements were performed on a HAAKE CABER 1 rheometer (Thermo Electron Corporation, WI). In these measurements, the solution was first loaded into a gap of 3 mm between two cylindrical plates with diameter of 6 mm, and then a 'necked' liquid bridge configuration was generated by rapidly separating two cylindrical plates to 9 mm at a constant strain rate of 0.3 m/s. The evolution of midpoint filament diameter, $D_{mid}(t)$ was then recorded as a function of time after cessation of motion of the plates. From these data, the Hencky strain, ε, and apparent extensional viscosity, $\overline{\eta}(\varepsilon)$, were calculated using equations 1 and 2, respectively [Anna and McKinley, 2001; McKinley et al., 2001]:

$$\varepsilon = 2\ln(\frac{D_0}{D_{mid}(t)}) \qquad (1)$$

$$\overline{\eta}(\varepsilon) = \frac{\gamma}{\dfrac{dD_{mid}(t)}{dt}} \qquad (2)$$

where D_0 is the initial diameter of the filament at its midpoint and γ is the surface tension of solution. The fluid elasticity was assumed to be dominated by the slowest relaxation process. The dependence of the filament diameter on time can then be described by employing a balance of the surface tension and elastic forces, as shown in equation 3 [Anna and McKinley, 2001; McKinley et al., 2001]:

$$D_{mid}(t) = D_0(\frac{GD_0}{\gamma})^{\frac{1}{3}}e^{-\frac{t}{3\lambda_c}} \qquad (3)$$

where G is the elastic modulus of the filament and λ_c is the longest relaxation time of the solution. The quantity GD_0/γ is referred as the elastocapillary number [Anna and McKinley, 2001].

2.3 Fiber characterization

Images of fibers were taken using a JEOL-6060 SEM (JEOL Ltd, Japan). Transmission electron microscopy (TEM) of fibers was performed in a JEOL JEM200 CX TEM microscope (JEOL Ltd, Japan). Wide-angle X-ray diffraction (WAXD) data were obtained using a diffractometer (Bruker) with CuKα radiation at 40 kV and 20 mA. Small angle x-ray scattering (SAXS) data were obtained using a copper microfocused x-ray beam generator (Osmic Inc., MI) operated at 45 kV and 0.66 mA. The sample to detector distance was 1.3 m as calibrated using a silver behenate standard. Two-dimensional SAXS data were collected using a multi-wire detector (Molecular Metrology Inc., MA). Measurements of glass transition temperature (T_g) were carried out using a Q1000 differential scanning calorimeter (TA Instrument, Inc., DE) at a heating rate of 10°C/min. T_g was determined based on the second heating scan preceded by a cooling scan at the same rate. Thermal stability of electrospun fibers was performed using a TA thermogravimetric analyzer (TA Instrument Inc., DE) at a heating rate of 20°C/min. Dynamic light scattering (DLS) measurements were performed on a BI-9000AT spectrometer (Brookhaven Instrument Corp., NY). The nanocomposite dispersions of 0.5% by weight in DMF were centrifuged using a Centrifuge 5804R (Eppendorf AG, Germany) at 5000 rpm for 15 mins. The top portion of solution was taken out by a syringe and filtered using 0.1 μm Puradisk^{TM} PTFE filter (Whatman plc, UK) for DLS measurements. The 5050-copolymer of 0.5% by weight in DMF was also used for DLS measurement.

3. RESULTS AND DISCUSSION

3.1 Material Characterization

3.1.1 DSC analysis of copolymers

Figure 1 displays the DSC thermographs obtained from the second heating scan for the poly (MMA-co-MAA) copolymers of various compositions. A single T_g is observed for all the copolymers, and the transition temperature increases with increasing MAA content. The observation of a single T_g clearly indicates that these copolymers are miscible at least on the scale of thermal conduction length during a DSC run, on the order of 20 to 40 nm [Huang and Chang, 2003].
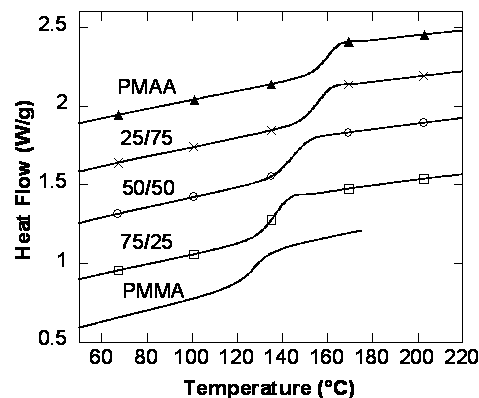

Figure 1. DSC thermographs obtained from the 2nd heating scan for PMMA, PMAA, and copolymers consisting of MMA and MAA monomers at a weight ratio of 75/25, 50/50, and 25/75.

3.1.2 X-ray diffraction analysis of nanocomposites

Wide-angle X-ray diffraction (WAXD) patterns obtained for the poly (MMA-co-MAA) nanocomposites consisting of MMT are shown in Figure 2a. No peaks are discernible for these MMT nanocomposites except for the PMAA-MMT nanocomposite. A diffraction peak at $2\theta = 5.74°$ is visible in the PMAA-MMT nanocomposite, corresponding to a d-spacing of 1.54 nm. In order to confirm the morphology of the MMT-containing nanocomposites without peaks in the WAXD, small angle x-ray scattering (SAXS) measurements were carried out. Figure 3 shows that no peaks associated with long-range order of clay structures are observed in SAXS for the MMT-containing nanocomposites. These data suggest that MMT clays are well dispersed in the as-polymerized MMT-nanocomposites, and they are predominantly exfoliated except for some tactoids with intercalated structure present in the PMAA-MMT nanocomposites. The WAXD patterns obtained for the corresponding FH-containing nanocomposites are shown in Figure 2b. In general, a diffraction peak at 2θ ranging from 7.45° to 8.50°, corresponding to a Bragg spacing of 1.04 to 1.19 nm, is observed. No peaks in SAXS are seen for these nanocomposites containing FH (not shown). These data suggest that clays are well dispersed in the FH-containing nanocomposites, yet they are predominantly intercalated in nature as indicated by the breadth of the WAXD peaks. Therefore, the as-polymerized MMT nanocomposites are exfoliated better than the corresponding FH-containing nanocomposites. MMT is a smectic clay consisting of layered aluminosilicate structures with lateral dimensions typically ranging from 0.1-1 μm, while FH is a synthetic, layered magnesium silicate with lateral dimensions around 4-5 μm, much larger than MMT [Gilman et al., 2000]. These results suggest that the particle size greatly affects the ease of exfoliation of clay in the nanocomposites, even in the presence of in situ emulsion

polymerization. For the purposes of electrospinning, the nanocomposites consisting of 50/50 weight ratio of MMA to MAA, denoted as 5050-copolymer nanocomposites, were selected in this work for the studies describe below.
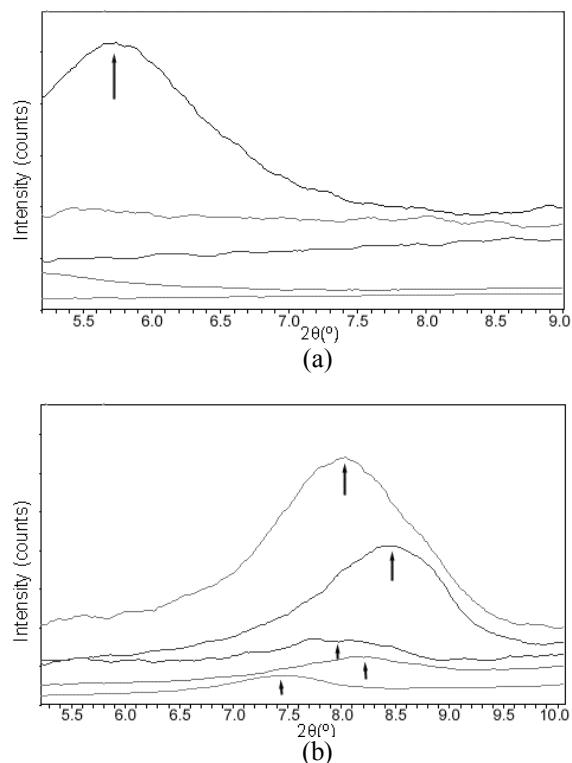

(a)

(b)

Figure 2. Wide angle x-ray diffraction patterns of nanocomposites, the polymer matrix from bottom to top: PMMA, copolymers consisting of 75/25, 50/50, 25/75 weight ratio of MMA to MAA, and PMAA: (a) MMT-containing nanocomposites, (b) FH-containing nanocomposites. The peak positions are indicated by the arrows.
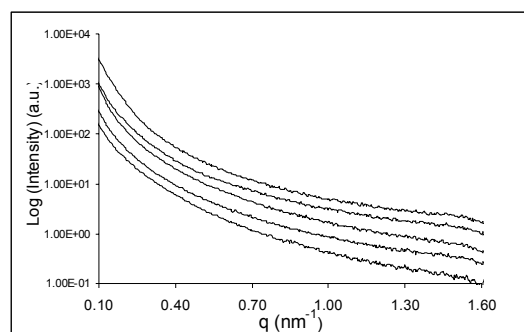

Figure 3. SAXS data for the nanocomposites containing MMT, the polymer matrix from bottom to top: PMMA, copolymers consisting of 75/25, 50/50, 25/75 weight ratio of MMA to MAA, and PMAA.

3.1.3 Rheology Analysis

3.1.3.1 Shear Rheology

When DMF was used as the solvent, a homogeneous translucent, gel-like dispersion was obtained for the 5050-MMT nanocomposite, while a white uniform dispersion was observed for the 5050-FH nanocomposite. Rheological measurements were carried out on these nanocomposite dispersions in DMF. Figure 4 shows steady shear viscosity as a function of shear rate. The dispersion of 5050-MMT in DMF exhibits higher zero-shear-rate viscosity than that of the neat 5050-copolymer solution and of 5050-FH dispersion. We used dynamic light scattering to determine the hydrodynamic diameter of the neat 5050-copolymer and the 5050-copolymer matrix in the nanocomposites. The latter was obtained by dissolving the nanocomposites in DMF and subsequently removal of the clay component through centrifuging and filtering. The results listed in Table 1 show that neat 5050-copolymer has the largest hydrodynamic diameter, followed by 5050-copolymer in the nanocomposite containing FH, and the least in the nanocomposite containing MMT. Since the DLS measurements were conducted using the same polymer concentration in DMF, the order of hydrodynamic diameters reflects the order of molecular weights. As a result, the increase in shear viscosity of nanocomposites dispersions is predominantly due to the presence of clay, and less dependent on the molecular weight of copolymers. At low shear rates (<50 s^{-1}, Figure 4), pronounced non-Newtonian shear thinning, which is characteristic of layered silicate ordering in the flow direction [Krishnamoorti et al., 2001], is observed in the 5050-MMT dispersion, but not in the 5050-FH dispersion. The latter exhibits predominantly Newtonian behavior, as also seen for the 5050-copolymer solution. The extent of shear thinning at these low shear rates has been reported to correlate directly with the concentration of platelets and the extent of filler-filler interaction [Wagener and Reisinger, 2003]. The particle size of FH is much larger than that of MMT; however, the effective anisotropy of the tactoids of FH may be compensated by the larger stack size or an intercalated silicate structure, indicated by WAXD, as compared to the tactoids of MMT. Based on this, our results from the steady shear rheological measurements suggest that MMT is more exfoliated than FH in the 5050-nanocomposite dispersions.
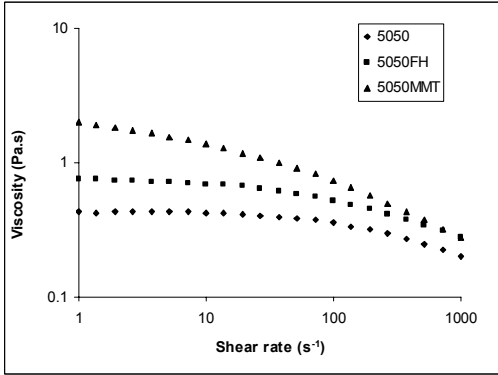
Figure 4. Comparison of shear viscosity vs shear rate of 5050-compolymer and their layered silicate nanocomposites.

Table 1: Comparison of hydrodynamic diameters of neat 5050-copolymer and 5050-copolymers in nanocomposites.

| 0.5 weight percent in DMF	Hydrodynamic diameter (nm)
Neat 5050-copolymer	21.24±0.38
5050-copolymer in FH nanocomposite	19.38±0.86
5050-copolymer in MMT nanocomposite	13.7±1.74

3.1.3.2 Extensional rheology and conductivity measurements

The time evolution of the midpoint diameter of the fluid filament during the extensional deformation was investigated for the 8 wt.% PMMA, 5050-copolymer and PMAA solutions, and the 5050-copolymer nanocomposite dispersions in DMF (Figure 5a). The capillary thinning of a fluid filament is a result of the competition of surface tension forces squeezing fluid from the filament and causing it to thin down, and polymer solution elasticity resisting extensional deformations [Anna and McKinley, 2001; McKinley et al., 2001]. A slower rate of capillary thinning is expected to correlate with better spinnability of the polymer solution. The data presented in Figure 5a shows that the PMMA solution has a lower rate of capillary thinning than the 5050-copolymer and PMAA solutions. The values of apparent extensional viscosity versus Hencky strain, calculated from the diameter vs. time data based on equations (1) and (2), are shown in Figure 5b. Strain hardening is seen in all the polymer solutions upon extensional elongation, and it is more pronounced in PMMA than in PMAA due to a higher molecular weight of PMMA (Mw=777,700 for PMMA and Mw=258,500 for PMAA based on gel permeation chromatography

measurements). In addition, results obtained from the conductivity measurement listed in Table 2 show that the PMMA solution has the highest conductivity compared to the 5050-copolymer and PMAA solutions in DMF. These observations would lead to the prediction of better electrospinnability for the PMMA solutions in DMF than for the 5050-copolymer and PMAA solutions, based on the expectation of a larger volume charge density from the conductivity measurement and a slower rate of capillary thinning from the extensional rheological analysis.
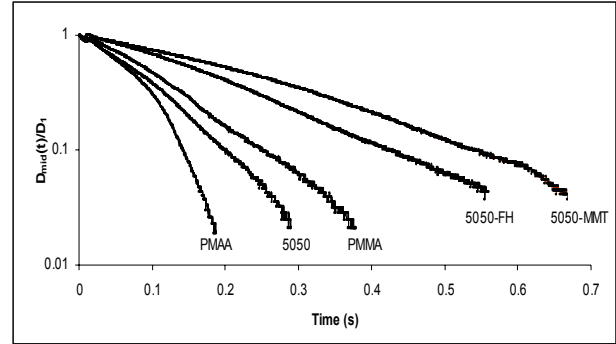
(a)
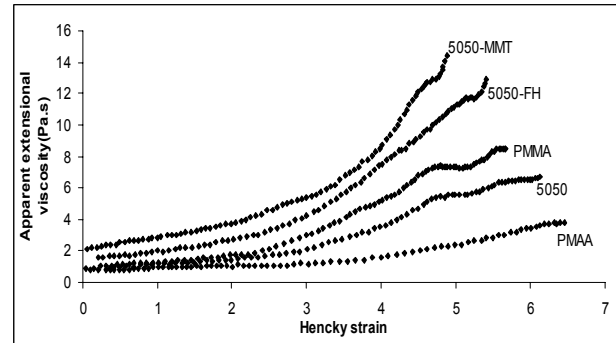
(b)

Figure 5. (a) Evolution of midfilament diameter vs time for the 5050-copolymers and their layered silicate nanocomposites (b) Apparent extensional viscosity vs Hencky strain for the corresponding materials.

Incorporation of clay apparently decreases the rate of capillary thinning of the nanocomposite dispersions as shown in Figure 5a, and strong strain hardening was observed for the 5050-MMT and 5050-FH dispersions (Figure 5b). Meanwhile, incorporation of clay does not cause a significant change in the conductivity of the nanocomposite dispersions (Table 2). As a result, the layered-silicate nanocomposite dispersions are expected to result in better electrospinnability than the corresponding polymer solutions. An elastic model, described by equation 3, was used to fit the data on extensional elasticity to determine the longest relaxation time, λ_c, associated with both polymer solutions and

nanocomposite dispersions [Anna and McKinley, 2001; McKinley et al., 2001]. Table 2 lists the values of the relaxation time, λ_c, and the filament break up time, t_b, obtained for these solutions and dispersions. Both the λ_c and t_b values associated with the nanocomposite dispersions are significantly higher than those of the unfilled polymers, presumably due to the results of filler-filler interaction and the polymer-filler interaction. In addition, the 5050-MMT dispersion exhibits a longer relaxation time and a longer experimental time to break than those obtained for the 5050-FH dispersion. We attribute this observation primarily to the difference in the extent of exfoliation of these clays, in accord with the results seen in the shear rheology analyses and WAXD patterns for as-polymerized nanocomposites.

Table 2. Values of longest relaxation time and time to break from extensional rheological measurements, and values of conductivity obtained for different solutions or dispersions.

8 wt% in DMF	λ_χ (s)	t_b (s)	Conductivity (μS/cm)
PMAA	1.18×10^{-2}	0.312	40.9
5050-copolymer	2.73×10^{-2}	0.337	79.6
PMMA	3.57×10^{-2}	0.442	112.0
5050-FH	5.38×10^{-2}	0.677	72.1
5050-MMT	6.96×10^{-2}	0.824	82.7

3.2 Electrospinning

Figure 6 shows the representative SEM images of electrospun fibers. At 6 wt.%, a bead-on-string morphology was observed when the 5050-copolymer (Figure 6a) and PMAA solutions were spun, while formation of fibers was achieved for the PMMA solution (Figure 6b), 5050-MMT (Figure 6c) and 5050-FH (Figure 6d) dispersions. Uniform fibers were obtained for the 5050-MMT nanocomposite (Figure 6c), but formation of inhomogeneities was visible on some of the electrospun 5050-FH fibers (Figure 6d). The latter is thought to be due to the dimension of the FH clays (about 4-5 μm) being significantly larger than the fiber diameter, resulting in large protrusions. Results of the TEM analysis indicate that the majority of intercalated FH structures are present in these inhomogeneities rather than in the uniform sections of the fibers. At 8 wt.% solutions, uniform fiber morphology was obtained for the PMAA, 5050-copolymer and PMMA solutions, and 5050-MMT dispersion (Figure 6e); however, protrusions were still observed on some of electrospun fibers from the 5050-FH nanocomposite dispersions (Figure 6f).
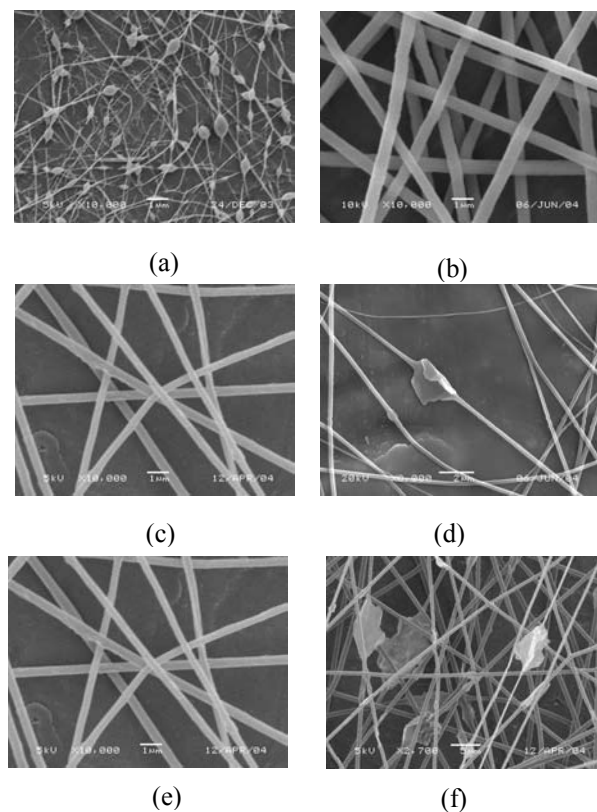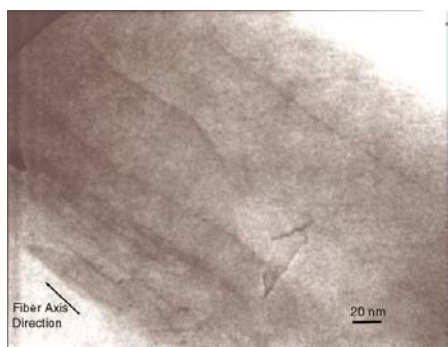

Figure 6. Representative SEM images of electrospun fibers from the following solutions in DMF: (a) 5050-copolymer (6 wt%), (b) PMMA (6%), (c) 5050-MMT (6%), (d) 5050-FH (6%), (e) 5050-MMT (8%), (f) 5050-FH(8%).

3.3 Characterization of fibers:

3.3.1 Morphology analysis

The morphology and the degree of dispersion of nanoclays within the fibers were characterized by TEM and wide-angle x-ray diffraction (WAXD). TEM results reveal that the majority of MMT platelets are exfoliated, and they are well distributed within the fiber and oriented along the fiber axis, as shown in Figure 7a. This clearly indicates the feasibility of electrospinning of the 2-D platelet structures and the potential to achieve proper alignment of these nanoclays along the fiber axis, which is critical for the nanocomposite fabrication. Fewer FH clay particles are observed within the as-spun fibers, and most of these appear to be in intercalated structures and reside near the edge of the fibers, as shown in Figure 7b. They are nevertheless well aligned in the fiber direction.

(a)
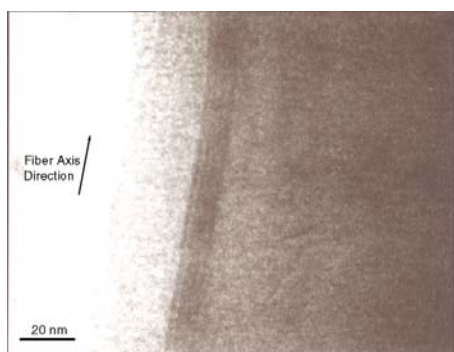
(b)

Figure 7. Representative TEM images of electrospun fibers from the following solutions in DMF: (a) 5050-MMT (6%), (b) 5050-FH (6%).

3.3.2 Thermal analysis of fibers

Thermal stability of the electrospun fibers was evaluated using TGA in nitrogen atmosphere. Figure 8 shows the weight change as a function of temperature at a heating rate of 20°C/min. The fibers spun from 5050-copolymer exhibit a shift of thermal degradation to higher temperatures relative to that of the PMMA fiber. An increase of about 100°C was noted in the 5050-copolymer and the corresponding MMT and FH nanocomposites; however, these fibers reveal noticeable weight loss at much lower temperature than the PMMA fiber. PMAA is hydrophilic, and a minor weight loss between room temperature and about 100°C may be due to the release of adsorbed water. Upon further heating, PMAA can undergo anhydride formation between pairs of carboxyl groups of the monomer units [Ho et al., 1992]. In the case of fibers electrospun from the 5050-copolymer containing materials, we expect weight loss from the formation of anhydrides between the carboxyl group of MAA and carboxylate group of MMA other than the release of adsorbed water and water from anhydride formation of MAA units. As a result, a broad, gradual weight loss prior to thermal degradation was seen in TGA data for these MAA-containing materials.

Figure 9 compares the residue of fibers after the TGA measurement; the 5050-MMT fibers charred after being heated above 650°C in nitrogen while a film

formation was noted in the 5050-FH fibers. The char formation indicates the presence of a percolated structure in the electrospun 5050-MMT fibers [Lee et al., 2002]. However, percolation is not evident from the TGA residue of 5050-FH fibers. The MMT char could act as an excellent insulator and mass transport barrier to mitigate subsequently the escape of volatile products generated during polymer decomposition. This char is desired to reduce the flammability and increase the self-extinguish property of nanocomposite fibers [Gilman et al., 2000].
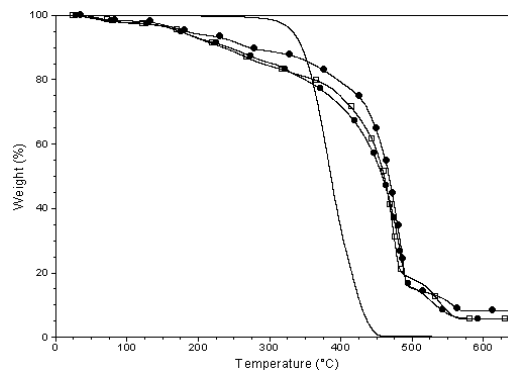

Figure 8. Comparison of weight changes of electrospun fibers as a function of temperature for PMMA (solid line), 5050-copolymer (♦), 5050-MMT (o), 5050-FH(!) nanocomposites.

(a)   (b)

Figure 9. Comparison of TGA residues of electrospun fibers: (a) 5050-MMT, (b) 5050-FH.

SUMMARY

Fibers of poly (MMA-co-MAA) copolymers and their layered silicate nanocomposites were prepared by electrospinning. The presence of MAA increased the T_g and thermal stability of the copolymers through formation of anhydrides upon heating. Incorporation of clays increased the zero-shear-rate viscosity of the nanocomposite dispersions over that of the pristine polymer solutions. The electrospinnability of copolymer solutions and nanocomposite dispersions predicted based on data from both extensional viscosity and conductivity measurements correlates well with the production of uniform fibers. Dispersion of clays within the nanocomposites improved the electrospinnability of these materials. Uniform fibers with diameters in the sub-micron range were obtained for the 5050-copolymer and 5050-MMT nanocomposite, while existence of

protrusions is observed from electrospinning of 5050-FH fibers, due to the large size of the FH clay platelets. MMT is predominantly exfoliated and well distributed within the fiber and along the fiber axis; however, fewer FH platelets are observed within the fiber and most of them appear to be intercalated. In addition, the fibers containing well-dispersed and predominantly exfoliated MMT clays char upon decomposition. Thus, through electrospinning of nanocomposite dispersions containing copolymers of MMA and MAA synthesized in situ with clays, novel fibers with high glass transition temperature, thermal stability, reduced flammability and increased self-extinguishing properties have been demonstrated.

ACKNOWLEDGEMENTS

REFERENCES

Doshi, J. and Reneker, D.H., 1995: Electrospinning Process of Electrospun Fibers, J. Electrostatics, **35** (2-3), 151-160.

Hohman, M.M., Shin, M., Rutledge, G.C. and Brenner, M.P., 2001: Electrospinning & Electrically Forced Jets, I. Stability Theory, Physics of Fluids, **13**, 2201-2220.

Hohman, M.M., Shin, M., Rutledge, G.C. and Brenner, M.P., 2001: Electrospinning and Electrically Forced Jets. II. Applications, Physics of Fluids, **13**, 2221-2236.

Reneker, D.H., Yarin, A.L., Fong, H. and Koombhongse, S., 2000: Bending Instability of Electrically Charged Liquid Jets of Polymer Solutions in Electrospinning, J. of Appl. Phys., **87**, 4531-4547.

Feng, J.J., 2002: The Stretching of An Electrified Non-newtonian Jet: A Model for Electrospinning, Physics of Fluids, **14**, 3912-3926.

Yarin, L., Koombhongse, S. and Reneker, D.H., 2001: Taylor Cone and Jetting From Liquid Droplets in Electrospinning of Nanofibers, J. Appl. Phys., **90**, 4836-4846.

Yu, J.H., Fridrikh, S.V. and Rutledge, G.C., 2004: Production of Submicron Diameter Fibers by Two-Fluid Electrospinning, Advanced Materials, in press.

Usuki, A., Kojima, Y., Kawasumi, M., Okada, A., Fukushima, Y., Kurauchi, T. and Kamigaito, O., 1993: Synthesis of Nylon 6-Clay Hybrid, J. Mater. Res., **8**, 1179-1184.

Kojima, Y., Usuki, A., Kawasumi, M., Okada, A., Fukushima, Y., Kurauchi, T. and Kamigaito, O., 1993: Mechanical Properties of Nylon 6-Clay Hybrid, J. Mater. Res., **8**, 1185-1189.

Giannelis, E.P., 1996: Polymer Layered Silicate Nanocomposites, Adv. Mater., **8**, 29-35.

Gilman, J.W., Jackson, C. L., Morgan, A.B., Harris, R., Manias, E. Giannelis, E.P. and Wuthenow, M., 2000: Flammability Properties of Polymer-Layered-Silicate Nanocomposites. Polypropylene and Polystyrene Nanocomposites, Chem. Mater., **12**, 1866-1873.

Wang, M., Singh, H., Hatton, A. and Rutledge, G.C., 2004a: Polymer, Field-Responsive Superparamagnetic Composite Nanofibers by Electrospinning, **45**, 5505-5514.

Fong, H., Liu, W., Wang, C.S. and Vaia, R.A., 2002: Generation of Electrospun Fibers of Nylon 6 & Nylon 6-Montmorillonite Nanocomposite, Polymer, **43**, 775-780.

Wang, M., Hsieh, A.J. and Rutledge, G.C., 2004b: Preparation of Nanofibers of PMMA-co-PMAA and PMMA-co-PMAA/clay Nanocomposites via Electrospinning, PMSE, ACS, **91**, 818-819.

Shin, M., Hohman, M.M., Brenner, M.P. and Rutledge, G.C., 2001: Electrospinning: A Whipping Fluid Jet Generates Submicron Polymer Fibers, Appl. Phys. Lett., **78**, 1149-1151.

Fridrikh, S.V., Yu, J.H., Brenner, M.P. and Rutledge, G.C., 2003: Controlling the Fiber Diameter During Electrospinning, Phys. Rev. Lett., **90**, 144502-1-4.

Anna, S.L. and McKinley, G.H., 2001: Elasto-capillary Thinning and Breakup of Model Elastic Liquids, J. Rheol., **45** (1), 115-138.

McKinley, G.H., Brauner, O. and Yao, M., 2001: Filament Stretching Rheometry and The Extensional Viscosity of Dilute and Concentrated Polymer Solutions Proc. 1st International Symposium on Applied Rheology, Korea, Jan. 18-19.

Huang, C.F. and Chang, F.C., 2003: Comparison of Hydrogen Bonding Interaction Between PMMA/PMAA Blends and PMMA-co-PMAA Copolymers, Polym., **44**, 2965-2974.

Krishnamoorti, R., Ren, J. and Silva, A.S., 2001: Shear Response of Layered Silicate Nanocomposites, J. Chem. Phys., **114**, 4968-4973.

Wagener, R. and Reisinger, T.J.G., 2003: A Rheological Method to Compare the Degree of Exfoliation of Nanocomposites, Polym., **44**, 7513-7518.

Ho, B.C., Lee, Y.D. and Chin, W.K., 1992: Thermal Degradation of Polymethacrylic Acid, J. Polym. Sci., Polymer Chemistry, **30**, 2389-2397.

Lee, H., Hsieh, A.J. and McKinley, G., 2002: Rheological Properties and Thermal Characteristics of Clay/ PMMA Nanocomposites, PMSE, ACS, **87**, 19-20